

Learning Dynamics: Group Project analyzing evolution game theory application in multiple myeloma cancer

Ayad Nouredine¹, Pierard Florian¹, Rodrigues Vitoria Joël¹ and Vercauteren Drubbel Alizée¹

¹Université Libre de Bruxelles (ULB). Master in Bioinformatics and Modeling
joerodri@ulb.ac.be
January 6, 2016

Abstract

In 2012, more than one and a quarter million people died from cancer in Europe (Eurostat, 2012). Thus understanding tumor growth and response to treatment is really promising to decrease this mortality. The pattern of somatic mutations leading to cancer is complex and this is one of the reasons why it is so difficult to study cancer. However it has been shown that tumor microenvironment plays a key role in cancer development and malignancy. Thus it would be useless to study cancers without paying attention to interactions with their microenvironments. The cytokines are, among other things, responsible for the interactions between malignant cells and normal cells. Interestingly these cytokines can be imagined as a process involving costs and benefits for the participating cells in a game pay-off matrix which has been well describe in terms of evolutionary game theory (EGT). This enables to capture the frequency-dependent nature of the system-dynamics. Here we show how the EGT can be applied to study the dynamics of the multiple myeloma bone disease (MM). According to Pacheco et al. (2014) we model different pathological scenarios and explore the different outcomes. Moreover, the concept of fitness introduced in the well-known replicator equation lets us compute the evolution of our cell populations. In this paper we show how the MM cell signals influence badly cancer prognosis. We model the effect of a bone marrow transplant and why it is important to combine bone marrow transplant and therapy. Finally we model the dynamic through a Moran birth death process, a stochastic dynamics in finite populations and compare if our previous discoveries and those from Pacheco et al (2014) are corroborated.

Introduction

Cancer

In Europe there were an estimated 3.45 million new cases of cancer (excluding non-melanoma skin cancer) and 1.75 million deaths from cancer in Europe in 2012 (Ferlay, et al., 2013). It thus represents a major concern worldwide. A cancer is a tumor that becomes malignant.

A tumor is an abnormal proliferation of cells that are not responding anymore to the regulatory signals. This leads to the formation of a mass which can be aggressive, invade the tissues, form metastasis and finally lead to death. In 2012, more than one and a quarter million people died from cancer

in Europe (Eurostat, 2012). Understanding tumor growth and response to treatment is a key element.

Cancer is the result of somatic mutation (gain of function or loss of function of a gene or both of them). The pattern of mutations leading to cancer is complex and this is one of the reasons why cancer is so difficult to study.

Unfortunately tumors are highly heterogeneous at several levels leading to a significant challenge to find effective therapies that target a wide variety of heterogeneous cancers without targeting the healthy tissues. However it has been shown that tumor microenvironment plays a key role in cancer development and malignancy. The advantage of the tumor microenvironment is that it conserves markers across different tumor types. Thus targeting the tumor microenvironment with appropriate designed therapies could be really promising (Ivey, Bonakdar, Kanitkar, Davalos, & Verbridge, 2015).

The interactions between the malignant cells and their environment are due to, among other things, the exchange of information in the form of cytokines. Following these observations we can imagine that the signaling process involves costs and benefits to the participant cells. From that moment, this can be converted into a game pay-off matrix for which the dynamics has been well described in term of evolutionary game theory (EGT)(Dingli, Chalub, Santos, Van Segbroeck, & Pacheco, 2009)(Pacheco, Santos, & Dingli, 2014).

The EGT allows us to explore cancer from brand new point of view. Biological signals are transformed into analytical data which can be computed and analyzed way quicker than what biology can do. Since years EGT has been used to model tumor evolution (Dingli, Chalub, Santos, Van Segbroeck, & Pacheco, 2009).

EGT represents an application of the game theory to model a biological issue, more precisely the evolution of a population. Compared to a classical game theory, the EGT doesn't take into account any strategy or anticipation. There is no notion of strategic choice in a cell population. Their fate only depends on their neighbors without any "rational choice".

In this article we reproduce the data obtained by Pacheco et al. which illustrate the utility of the application of EGT to cancer. Indeed we apply EGT to multiple myeloma bone disease (MM). This well-known form of cancer is characterized among other things, by bone loss. The generation of the first MM cell is a multistep process implying numerous mutations that lead to a transformation of a normal plasma cell into an MM cell (Bergsagel & Kuehl, 2005). Here we are interested

only in the dynamic process of clonal expansion of the MM cells. Accordingly we consider that the first MM cell has already appeared and that no new mutation will occur over time.(Pacheco, Santos, & Dingli, 2014)

Interestingly they discover that the bone marrow microenvironment is essential for the tumor cells clonal expansion and its survival. Here the microenvironment involves different populations including osteoblasts (OB) and osteoclasts (OC). The remodeling of the bone marrow microenvironment involved a balance between bone resorption mediated by OC and bone formation mediated by OB (Figure 1a). This dynamic balance is disrupted by the appearance of the MM population. Indeed, MM population is known to produce cytokines that recruit and activate OC, leading to a higher bone resorption and a potential disadvantage for OB cells (Figure 1b). Consequently symptoms appear only after a certain clonal expansion of the MM cell population and thus an increasing resorption. This dynamic can be capture in an EGT framework which provides a convenient way to represent the complex exchange of chemical signals between the different cell types (Figure 1c) into a pay-off matrix with costs and benefits for each cell type.(Pacheco, Santos, & Dingli, 2014)

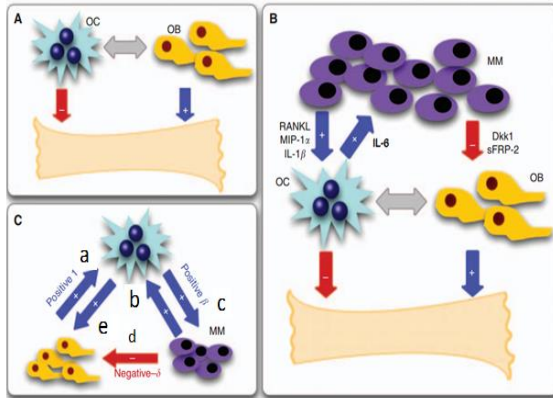


Figure 1: Normal and pathological bone turnover. (A) Bone homoeostasis assured by osteoblasts (OB) and osteoclasts (OC). (B) The presence of multiple myeloma cells (MM) disturbs bone homoeostasis by cytokine production that recruit and activate OC cells, increasing bone resorption. OC produce growth factors for MM cells, which also secrete cytokines that suppress OB activity. (C) The effect of each cytokines on another population can be summarized in costs and benefits attributed to the letters a,b,c,d and e. (Dingli, Chalub, Santos, Van Segbroeck, & Pacheco, 2009).

Computation of evolution game theory

To compute this system, we have to consider MM cells as cells that attempt to overcome OB cells. To describe this type of interaction the replicator equation (RE) is used as the central equation of our EGT. The RE uses the concept of fitness of cell types but doesn't incorporate the concept of mutation. In our case, as said before, we won't consider any apparition of a new mutation during the evolution of the outcome. Thus the outcome depends only on the initial conditions and the proportion of each population. It can be

seen as a selection between 3 species fighting for a same spot and interacting with each other.

The influence of a cell type on another one can be introduced in a pay-off matrix to compute the RE. We have to adapt parameters to fit the best our model. Thereby, Pacheco et al. introduce parameters in the pay-off matrix that stand for the interactions between the 3 cell populations (1.1)(Figure 1c). (Pacheco, Santos, & Dingli, 2014)

$$\begin{array}{c} OC \\ OB \\ MM \end{array} \begin{array}{ccc} OC & OB & MM \\ \left[\begin{array}{ccc} 0 & a & b \\ e & 0 & -d \\ c & 0 & 0 \end{array} \right] \end{array} \quad (1.1)$$

Another matrix (1.2) results from the first one by simplifying the parameters. The transformation in the simplified matrix considers that $a = e$, $\beta = c/e$ and $\delta = dc/be$. β represents the ratio between stimulation of MM by OC and stimulation of OB by OC. δ represents the ratio between the negative and positive feedback of the OB. This reduction corresponds to a projective transformation of the relative frequencies. As stated by (Hofbauer & Sigmund, 1998), this transformation changes the position of the stability points, but not their nature. Thus this reduced model can be used to study the dynamics and comparing different scenarios between them (Pacheco, Santos, & Dingli, 2014).

$$\begin{array}{c} OC \\ OB \\ MM \end{array} \begin{array}{ccc} OC & OB & MM \\ \left[\begin{array}{ccc} 0 & 1 & \beta \\ 1 & 0 & -\delta \\ \beta & 0 & 0 \end{array} \right] \end{array} \quad (1.2)$$

Using this matrix (1.2), we obtain 3 differential equations, one for each type of cells. With these equations we can observe the trend of each cells population depending of the other. The evolution of each cell type depends of the initial frequency of each one and the values of β and δ . A simplex plot, also known as ternary plot, can show the tendency of each population to reach a stable point.

For our analysis, we have to consider that the total size of the population is conserved and that population cells number are frequencies. The sum of all 3 frequencies (OC, OB, MM) will always be equal to 1. So knowing 2 cell frequencies we can deduce the last one.(Pacheco, Santos, & Dingli, 2014)

As an extension to this work, our team decided to verify if after applying a finite population model, the general conclusions that have been taken from the above models stay the same. The advantage of our study is that even a less fit cell population has still a chance to replace a fitter cell type. This is interesting to study because it could show that only blocking a part of the MM signals could be sufficient to change the fate of the disease.

Methods

The replicator equation

In this work, we used the well-known RE (Taylor & Jonker, 1978) to compute the evolution of our 3 cells types. The parameters of the equations depend on the pay-off matrix (Pacheco, Santos, & Dingli, 2014).

We obtain 3 derivatives for each cell types:

$$\frac{dx_i}{dt} = x_i(t)[\varphi_i(x_1, x_2, x_3) - \varphi_{avg}] \quad (i = 1, 2, 3)$$

The fitness of each cell type is equal to the sum of every pay-offs of the row of a cell type multiplied by the row frequency and by the column frequency.

$$\varphi_i(x_1, x_2, x_3) = \sum_{k=1}^3 A_{ik} * x_k$$

E.g., the fitness of OC is equal to:

$$A_{11} * f_1(t) * f_1(t) + A_{12} * f_1(t) * f_2(t) + A_{13} * f_1(t) * f_3(t)$$

Where $f_i(t)$ is the relative frequency of each cell type: $f_1(t)$ for OC cells, $f_2(t)$ for OB cells and $f_3(t)$ for MM cells.

The average fitness of the population represents the average fitness of a given system. It is always the same for a definite pay-off matrix. It's the sum of every pay-off multiplied by its column and row frequencies:

$$\varphi_{avg} = \sum_{i=1}^3 \sum_{k=1}^3 x_i * A_{ik} * x_k$$

Also note that in this model, the position of the saddle point that might emerge in a simplex plot (projection of the OC-OB-MM frequencies on an equilateral triangle), can be calculated as such:

$$q^* = \left(\frac{\delta}{1 + \delta + \beta(\delta + \beta - 2)} \right), \left(\frac{\beta(\delta + \beta - 1)}{1 + \delta + \beta(\delta + \beta - 2)} \right), \left(\frac{1 - \beta}{1 + \delta + \beta(\delta + \beta - 2)} \right)$$

Calculations and plotting of results

Two approaches were used for the plotting and the verification of the results from Pacheco et al. (2014).

Simplex plots and contour maps: Since the replicator equation is a nonlinear ordinary differential equation, the only way to plot the different values for a simplex plot is to use a numerical solver algorithm. After research on possible candidates for this job, our gaze fell upon *Dynamo3S* (Sandholm, Dokumaci, & Franchetti, 2012), a script notebook for *Wolfram Mathematica*. While the code is open-source, sadly the *Mathematica* is a closed-software programming environment used for complex calculation task.

This being said, *Dynamo 3S* was developed for the simple computation and plotting of classical game theory problems. By parameterizing the algorithm, such as defining the payoff matrix, the type of dynamic function (in our case a RE) and

other graphical parameters, we were able to reproduce the simplex plots shown in Pacheco et al. (2014).

Generation of discrete game scenarios: In an attempt to simulate ourselves how the population fractions would evolve when playing a game as defined by the game matrix, we wrote a Python script that uses the methodology described for the replicator equation. But instead of using a continuous version, discrete calculations were operated, which recalculated the population frequencies based on the fitness values as described above. These results were then plotted as to show how the ratio OB/OC evolves with the fraction of MM in the population. The exact algorithm was worked out by studying a previous article (Dingli, Chalub, Santos, Van Segbroeck, & Pacheco, 2009) and by consulting with a student group that was working on that very same article (Georges Coppin, pers. Communication).

Finite vs infinite population model

All the models stated before work under the assumption of infinite populations, as to satisfy the condition that the strategy frequencies are representative. We thus chose to test whether the conclusion based on the EGT model remains valid in a finite population model (Pacheco, Santos, & Dingli, 2014).

To study the dynamics in finite populations, one might use a Moran process (birth-death process). First described by Moran (Moran, 1962), it has since been used to analyse various EGT scenarios, namely in studies relating to the emergence of cooperation (Imhof, et al., 2005 ; Fudenberg & Imhof, 2006 ; Han, et al., 2013). The basis of the model can be described as such: starting from a population of size N , with each individual adhering to one of the studied strategies. At each time step, i.e. generation, we use a pairwise comparison rule (Traulsen, et al., 2006), meaning that randomly chosen individuals will face each other pairwise. In a classical EGT scenario, the individual with the highest fitness (payoff) would replace the less fit one with a probability of $p = 1$. But, in this model, the probability will be calculated using Fermi function:

$$\frac{1}{1 + e^{-\beta * (fa - fb)}}$$

In this case fa and fb can be replaced by the payoff values for the given strategies. In this scenario, even a less fit individual has a chance to replace a fitter individual. The β parameter describes the “temperature” or “the selection strength”. As $\beta = 0$, the replacement process is random and corresponds to neutral drift. As β tends to ∞ , the process becomes more and more deterministic, tending to the normal EGT scenario described before. Without mutations, these populations evolve towards monomorphic states: once a strategy becomes fixated, i.e. each individual has the same strategy, the population can't escape from this state.

But, if we suppose low mutation rates (change of strategies), a given individual can randomly change strategy, leading to a different dynamic. This dynamic can be described by a reduced Markov chain, where the transition probabilities indicate the fixation probability of a single mutant in a population dominated by the other state. Each state describes a monomorphic population, for which a stationary distribution

can be calculated, indicating how much time the population spends in that state.

In our case we adapted the methodology from (Han, Pereira, Santos, & Lenaerts, 2013). Lenaerts, T, one of the original authors, was so kind as to share with us a C++ program that allows to calculate the dynamics described here above. The code was modified as to represent the scenario described for the three cell types (OC, OB, MM). Several payoff matrices of interest were ran through this code, each time comparing the results for a population size $N = 100$ and $N = 10000$. Because computational time grew substantially with population size, we refrained from larger population size, but insisting on the fact that with larger population sizes the observed dynamics should near those of infinite populations. Furthermore, the simulations were ran with $\beta = 0.1$, as to simulate a scenario where fitness has a more marginal effect on replacement of a given cell-type.

Result

Increasing Delta lead to a significant impact on life history

Increasing δ for fixed β increases the disadvantage of OB cells in the presence of MM cells. For β value fixed at 2 we have study the influence of different values of δ in the payoff matrix 1.2 ($\delta=0$, $\delta=1/3$, $\delta=1$ and finally $\delta=10$). Consequently a considerable bone loss appears without a significant increase in the MM population (Dingli, Chalub, Santos, Van Segbroeck, & Pacheco, 2009).

As we can see in figure 2, the only stable equilibrium is the co-existence of MM and OC. Nevertheless, changes in δ may have a significant effect on the life history of the disease and

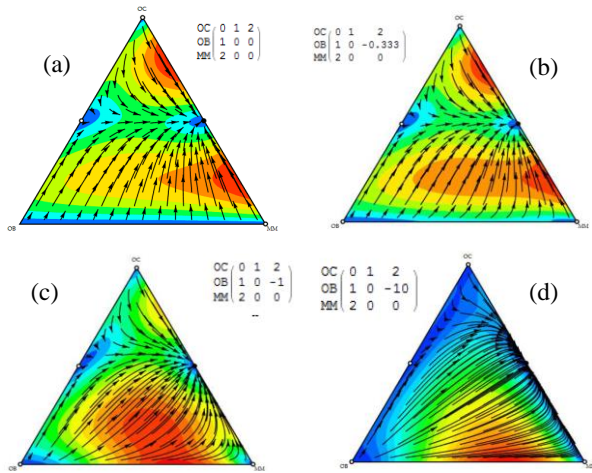


Figure 2: The effect of increasing δ on the dynamic evolution of multiple myeloma (MM, right peak of triangle), osteoblast (OB, left peak) and osteoclasts (OC, upper peak) cell type. (a) One need not postulate a negative effect of MM on OB even if $\delta=0$ (MM and OB are neutral with respect to each other). (b), (c) and (d) show that δ affects the path and progression time between OB-OC and also OC-MM equilibrium. OB-OC equilibrium was disturbed by introducing one MM cell for different values of δ (Dingli, Chalub, Santos, Van Segbroeck, & Pacheco, 2009).

associated progression time, as shown in figure 2d, the length of the arrows increases and they point towards the only stable equilibrium OC-MM. This may explain the example of myeloma-induced osteoporosis without a massive MM cell burden. Similarly, when we increase the net benefit that OC cells obtain from MM higher than what they get from OB cells, β will increase leading to more bone destruction, higher tumor burden and faster tumor progression.

Analysis of the effect of bone marrow transplant

β represents the ratio between MM stimulation and OB stimulation. So higher β is, higher the ratio MM/OB will be and so the outcome will be worse.

In normal condition, β is higher than 1 meaning that stimulation of MM cells is higher than stimulation of OB cells by OC cells. It leads to a bad prognosis where OB cells disappeared to increase OC and MM cells proportions (50% both). Here we show the evolution of the 3 cell populations in a simplex (Figure 3a) and the ratio OB/OC combined with the proportion of MM along the generations (time) (Figure 3b). The ratio OB/OC cells will tend to 0 after some generations because the OB will tend to 0. Then we observe the effect on a bone marrow transplant (BMT) in the outcome of the disease (Figure 3c).

Thanks to a BMT, we almost “reset” the proportion of each cell population. But with only 1 MM cell, we can’t reach a state of 50% OB and 50% OC because this state is a saddle point (empty dot) and so isn’t stable. The population will tend to its only stable point (black dot) where OB disappears (Figure 3a). So in normal condition, the BMT will only postpone the death (3c).

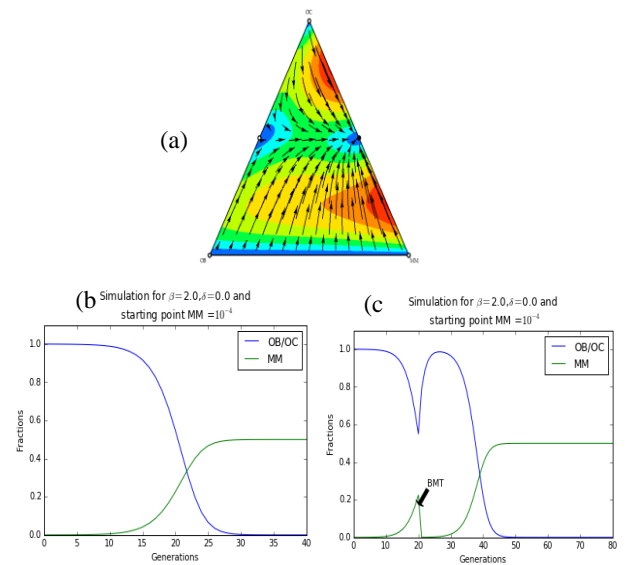


Figure 3: Analysis of the outcome of populations where $\beta = 2$ and $\delta = 0$. a) Simplex of the evolution of the populations without any BMT where MM is the right peak, OB the left peak and OC the upper peak. b) The evolution of the population without any BMT represented by a 2D graph and c) the evolution of the populations with a BMT. The blue curve shows the OB/OC ratio dynamic and the green one shows the MM dynamic.

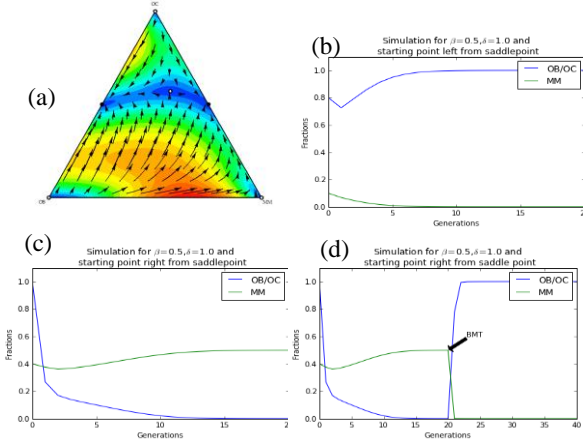


Figure 4: Analysis of the outcome of population where $\beta = \frac{1}{2}$ and $\delta = 1$. a) Simplex showing the global evolution where MM is the right peak, OB the left peak and OC the upper peak. b) Evolution starting from left from the saddlepoint c) Evolution starting right from the saddlepoint. d) We observe a curative BMT even if we start at the right of the saddle point. The blue curve shows the OB/OC ratio dynamic and the green one shows the MM dynamic.

By giving a drug treatment, we can change the β of the system. We can decrease β by either decreasing MM stimulation or increasing OB stimulation. The easiest way is to inhibit MM stimulation with the drug. When β is lower than 1 the stability of the system changes and we can observe 2 stable points (black dots) and a saddle point (empty dot) (Figure 4a). The first stable point is the healthy one where OB and OC are both at 50% and we have no MM. The unhealthy stable point is the same as with β higher than 1. In this case MM and OC are both at 50% and we have no OB. So now we observe that if we start at the left of the saddle point, so with a globally lower MM proportion, we will tend to the healthy stable point (Figure 4a). But if we start from the right of the saddle point, so with a globally higher MM proportion, we will tend to the unhealthy stable point which leads to the death (Figure 4b).

After drug treatment we have a shift between a state where the only stable point is an unhealthy one and a state where there are an healthy and an unhealthy stable point. In this new state, a BMT allows a shift to the left of the saddle point, leading to the proportions where the stable point is the healthy one without any MM and with 50% OB and 50% OC (Figure 4d).

Finite population analysis

After running several payoff scenarios through the Moran process simulation, we obtained the transition probabilities and the stationary distributions (Annexes: table 1). In both scenarios where we added a disequilibrium in the OC-OB

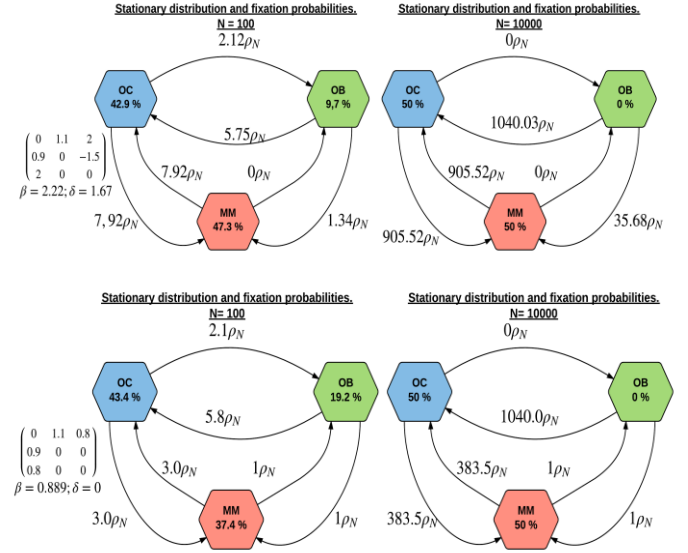


Figure 5: Illustration of the results from the Moran process for scenarios where $a \neq e$. ρ_N represent the neutral drift, which is proportional to $1/N$. Fermi function selection parameter equals 0.1.

homeostasis (i.e. $a \neq e$), the final stationary distributions tend toward a favouritism of OC and MM cells (figure 5). In the first one, where $\beta = 2.22$ and $\delta = 1.67$, we observe that for $N = 100$ the population stays 43 % of the time in a monomorphic OC state and 47% in a MM state. This tendency is accentuated in the $N = 10000$ simulation, where the population stays 50% of the time in the OC or the MM. In the second scenario ($\beta = 0.889$ and $\delta = 0$), the overall tendencies are the same. But looking at the transition probabilities, some differences appear between the two scenarios. In the first one, there are higher transitions from OB to OC and OB to MM, indicating that both effects (disequilibrium in homeostasis of OC and OB, as well as a positive δ) seem to structure the final distributions of each monomorphic state. In the second scenario, even in the absence of a δ value, so no negative effect of MM cells on OB cells, the transition from OB to OC stays dominate.

When looking at scenarios that reflect more the ones studies in (Pacheco, Santos, & Dingli, 2014), the results differ quite a bit (figure 6). When using a payoff matrix that generates a $\beta + \delta > 1$, the respective distribution for $N=100$ are OC= 28.1 %, MM = 57.9 % and OB = 14.0 %. Furthermore, the only transition probability pair that isn't equilibrated is the one between OB and MM, showing a net transition probability of $8.0\rho_N$ from OB to MM. For $N = 10000$, the transition probabilities are globally higher, but the tendencies stay the same. But we observe a shift in the stationary distributions, which become are OC= 32.5 %, MM = 37.6 % and OB = 29.9 %.

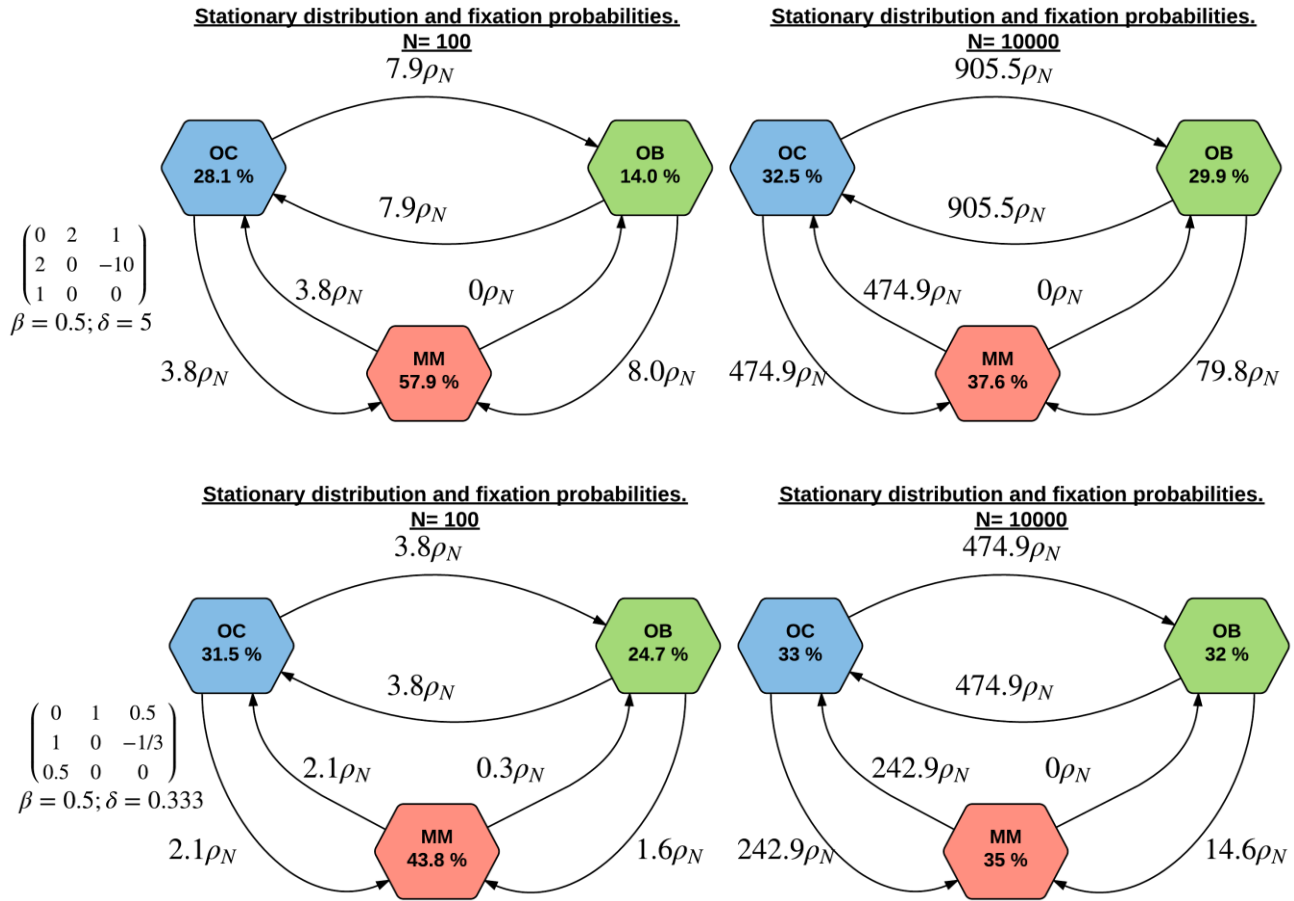


Figure 6: Illustration of Moran process results. Upper scenario shows a situation where $\beta + \delta > 1$. The lower scenario shows a situation where $\beta + \delta < 1$. ρ_N represent the neutral drift, which is proportional to $1/N$. Fermi function selection parameter equals 0.1.

In the second scenario we tested a case where $\beta + \delta < 1$. For $N=100$, the distributions are OC= 31.5 %, MM = 43.8 % and OB = 24.7%, indicating here again a slight favoritism for MM and OC cells. The same can be said for the transition probabilities, which are equilibrated, expect the transition probability from OB to MM, having a net tendency of $1.6-0.3 = 1.3\rho_N$. For $N = 10000$, the results indicate a disappearance of the observed distributions, the Markov chain indicating now OC= 33 %, MM = 35 % and OB = 32 %. Nevertheless, the transition probability between OB and MM is now $14.6\rho_N$.

Here we have studied the application of EGT to multiple myeloma bone disease both in an infinite population and in a finite population.

As we observe, changing the ratio between negative and positive feedback (δ) has only an effect on the speed of the outcome and consequently a bad prognosis. So to find a treatment we have to focus on the ratio between MM stimulation and OB stimulation (β).

Treatment of the disease

BMT consists on a transfer of a healthy bone marrow from a donor to the unhealthy patient with high MM population. When it is possible, the transplant is done to itself, it is called an autologous transplant. This type of transplant avoids any rejection problem and still reduces the burden of the disease. In normal condition, where the stimulation of MM by OC is higher than stimulation of OB by OC (β), the prognosis is bad because the only stable point of the system is when OC and MM are both at 50%. When using BMT the MM charge is substantially reduced. But even with a very low MM cell

Discussion

Cancer is responsible of numerous deaths around the world. Because of its huge heterogeneity inter-tumoral together with intra-tumoral, it is a disease really difficult to cure. Actually the only therapy that cures from cancer is the entire resection of the tumor. This is why better understanding cancer is a really promising field. One way to further our knowledge of cancer biology is evolutionary game theory scenarios mimicking a malignant population dynamic.

count, we can't reach a state of 50% OB and 50% OC because it corresponds to an unstable saddle point. The population will tend to its only stable point where OB disappears (Figure 3a). So in normal condition, the BMT will only postpone the death (3c).

After drug treatment (e.g. decreasing the stimulation of MM cells by OC) we have a shift from a state where the only stable point is an unhealthy one (Figure 3a) to a state where there are a healthy and an unhealthy stable point (Figure 4a) (Pacheco, et al., 2014). In this new state, a BMT can be curative by shifting from the right of the saddle point to the left. The cell populations will thus tend to the stable point where OB and OC are both at 50% and there is no MM (Figure 4d).

Finite population model

The results obtained from the finite population model proposed in this article couldn't corroborate the results obtained by (Pacheco, Santos, & Dingli, 2014) with their infinite population EGT approach. Indeed, as shown in the results section, we should have expected an equilibrium state between OC-OB for cases were $\beta + \delta < 1$ (figure 6). This situation describes a biological environment where the stimulation ratio for OC-MM is lower than OC-OB and where the negative impact ratio from MM on OB is lower than the stimulation of OC-OB. Thus, one should expect that the MM cells should have a low probability of establishing a high population count. Yet, especially in the case of $N = 100$, the MM cells seem favored, indicating that in a small (sub)population the stochastic effects of this model allows for a MM population to set foot. Even when increasing the population size, which should approach a more deterministic scenario, we do not obtain a tendency towards an OC-OB equilibrium, even though the Markov chain shows a more balanced stationary distribution.

The same strange behavior is observed for the $\beta + \delta > 1$ scenario. Here we should expect a clear dynamic favoring the establishment of a MM-OC equilibrium, yet while this seems to be the case for $N = 100$, the stationary distribution stabilizes for $N = 10000$.

This begs the question as to why the general tendencies in an EGT infinite population model are not replicated. An hypothesis could simply be the fact that the model applied here isn't sufficient to describe the biological dynamics of multiple myeloma. It is possible that the selection factor chosen for the Fermi function ($\beta = 0.1$) was too low as to represent the selective pressure underlining the real biological process. We also know that the establishment of a MM population requires a favorable microenvironment and that the MM cell stage is preceded by an asymptomatic MGUS (monoclonal gammopathy of undetermined significance) (Roodman, 2009; Pacheco, Santos, & Dingli, 2014). In this case, the assumption that the mutation rate is low could be questioned, since the transformation from a well-established MGUS to MM could be rather high.

We also modeled a scenario where the equilibrium between OC-OB is already disturbed, as can be supposed in pathologies as rheumatoid arthritis (Tanaka, Nakayamada, & Okada, 2005) or other forms of deregulation such as changing estrogen levels during menopause or hyper inflammatory

reactions (Mundy, 2007). As shown (figure 5), even in a low population size, the dynamic tends towards a higher percentage of OC and MM. Increasing the population size confirms this by producing a distribution of OC = 50 %, MM = 50 % and OB = 0 %. So in this case we obtain these expected symptoms, namely a high OC and MM count, which accounts for the osteoporosis observed in patients suffering of multiple myeloma. Nevertheless, while this example helps to illustrate how certain patients, showing this unfavorable preconditions, could be more susceptible to MM and could show a faster disease evolution, it moves away from the conditions set in the Pacheco et al. model. Indeed, their model presupposes that the payoff matrix for OB vs OC is of the coexistence type, meaning that both obtain the same payoff. Thus, these results do neither corroborate nor refute their findings, but is more of an extended case study.

Supplementary files

Cancer_game.py : Python script used to generate discrete population simulations

Game_cancer_moran.cpp : modified C++ code, used to calculate stationary distribution and transition probabilities.

Final_results.odt : calculation sheet containing raw data obtained from Game_cancer_moran.cpp

References

- Bergsagel, P., & Kuehl, W. (2005, Sep 20). Molecular pathogenesis and a consequent classification of multiple myeloma. *J Clin Oncol.*, 23(26), 6333-8.
- Dingli, D., Chalub, F., Santos, F., Van Segbroeck, S., & Pacheco, J. M. (2009). Cancer phenotype as the outcome of an evolutionary game between normal and malignant cells. *British Journal of Cancer*, 101(7), 1130-1136.
- Eurostat. (2012). *Cancer statistics*. Retrieved from http://ec.europa.eu/eurostat/statistics-explained/index.php/Cancer_statistics#Deaths_from_cancer
- Ferlay, J., Steliarova-Foucher, E., Lortet-Tieulent, J., Rosso, S., Coebergh, J., Comber, H., . . . Bray, F. (2013). Cancer incidence and mortality patterns in Europe: estimates for 40 countries in 2012. *European Journal of Cancer*, 49(6), 1374-1403.
- Fudenberg, D., & Imhof, L. A. (2006). Imitation processes with small mutations. *Journal of Economic Theory*(131), 251-262.
- Han, T. A., Pereira, L. M., Santos, F. C., & Lenaerts, T. (2013). Good Agreements Make Good Friends. *Scientific Reports*, 3, 2695.
- Hofbauer, J., & Sigmund, K. (1998). *Evolutionary Games and Population Dynamics* (Vol. First edition). Cambridge, UK: Cambridge University Press.

- Imhof, L. A., Fudenberg, D., & Nowak, M. A. (2005). Evolutionary cycles of cooperation and defection. *PNAS*, 102(31), 10797-10800.
- Ivey, J., Bonakdar, M., Kanitkar, A., Davalos, R., & Verbridge, S. (2015). Improving cancer therapies by targeting the physical and chemical hallmarks of the tumor microenvironment. *Cancer Letters*, S0304-3835(15).
- Moran, P. A. (1962). *The statistical processes of evolutionary theory*. Claredon Press.
- Mundy, G. R. (2007). Osteoporosis and Inflammation. *Nutrition Reviews*, 65, 147-151.
- Pacheco, J. M., Santos, C. F., & Dingli, D. (2014). The ecology of cancer from an evolutionary game theory perspective. *Interface Focus*, 4.
- Roodman, G. D. (2009). Pathogenesis of myeloma bone disease. *Leukemia*, 23(3), 435-441.
- Sandholm, W., Dokumaci, E., & Franchetti, F. (2012). *Dynamo: Diagrams for Evolutionary Game Dynamics*. Retrieved 12 11, 2015, from <http://www.ssc.wisc.edu/~whs/dynamo>.
- Tanaka, Y., Nakayamada, S., & Okada, Y. (2005). Osteoblasts and osteoclasts in bone remodeling and inflammation. *Curr Drug Targets Inflamm Allergy*, 4(3), 325-328.
- Taylor, P., & Jonker, L. (1978). Evolutionarily stable strategies and game dynamics. *Mathematical Biosciences*, 40, 145-156.
- Traulsen, A., Nowak, M. A., & Pacheco, J. M. (2006). Stochastic dynamics of invasion and fixation. *Phys. Rev. E*(74), 011909.

Annexes

Table 1: Summary of all values obtained from a Moran process simulation. The beta parameter for the Fermi function was $\beta = 0.1$. Parameters indicate the chosen payoff values; Beta and delta indicate the calculated stimulation ratios; Column 4-9 indicate the fixation probabilities of a given mutant in a given population (in respects to the neutral drift); the last columns describe de fixation probabilities.

Pop. Size	Parameters [a,b,c,d,e]	Beta; Delta	OB in OC	MM in OC	OC in OB	MM in OB	OC in MM	OB in MM	prop OC	prop OB	prop MM
100	[1.1,2,2,-1.5,0.9]	2.2; 1.67	2,12	7,92	5,75	3,59	7,92	0,00	0,43	0,10	0,47
	[4,2,2,-1.33,4]	0.5; 0.33	15,69	7,92	15,69	2,93	7,92	0,00	0,32	0,27	0,42
	[1.1,0.8,0.8,0,0.9]	0.89; 0	2,12	3,03	5,75	1,00	3,03	1,00	0,43	0,19	0,37
	[2,1,1,-10,2]	0.5; 5	7,92	3,75	7,92	8,01	3,75	0,00	0,28	0,14	0,58
	[1,0.5,0.5,-0.33,1]	0.5; 0.33	3,75	2,10	3,75	1,57	2,10	0,30	0,32	0,25	0,44
10000	[1.1,2,2,-1.5,0.9]	2.2; 1.67	0,00	905,52	1040,03	35,68	905,52	0,00	0,50	0,00	0,50
	[4,2,2,-1.33,4]	0.5; 0.33	3295,44	905,52	3295,44	29,14	905,52	0,00	0,33	0,33	0,34
	[1.1,0.8,0.8,0,0.9]	0.89; 0	0,00	383,49	1040,03	1,00	383,49	1,00	0,50	0,00	0,50
	[2,1,1,-10,2]	0.5; 5	905,52	474,90	905,52	79,79	474,90	0,00	0,33	0,30	0,38
	[1,0.5,0.5,-0.33,1]	0.5; 0.33	474,90	242,89	474,90	14,57	242,89	0,00	0,33	0,32	0,35